ELSEVIER

Contents lists available at ScienceDirect

Biochimica et Biophysica Acta

journal homepage: www.elsevier.com/locate/bbadis



Classical transient receptor potential 6 (TRPC6) channels support myofibroblast differentiation and development of experimental pulmonary fibrosis



Katharina Hofmann ^a, Susanne Fiedler ^a, Sarah Vierkotten ^b, Jonas Weber ^a, Stephan Klee ^b, Jie Jia ^c, Wolfgang Zwickenpflug ^a, Veit Flockerzi ^d, Ursula Storch ^a, Ali Önder Yildirim ^c, Thomas Gudermann ^a, Melanie Königshoff ^b, Alexander Dietrich ^{a,*}

- a Walther-Straub-Institute of Pharmacology and Toxicology, Member of the German Center for Lung Research (DZL), University of Munich, Munich, Germany
- b Research Unit Lung Repair and Regeneration, Comprehensive Pneumology Center, Member of the German Center for Lung Research (DZL), Munich, Germany
- ^c Comprehensive Pneumology Center (CPC), Institute of Lung Biology and Disease, Member of the German Center for Lung Research (DZL), Helmholtz Zentrum, Munich, Germany
- ^d Experimental and Clinical Pharmacology and Toxicology, Saarland University, Homburg, Germany

ARTICLE INFO

Article history: Received 14 July 2016 Received in revised form 28 November 2016 Accepted 4 December 2016 Available online 6 December 2016

Keywords: TRPC6 TGF-β1 Pulmonary fibrosis Cell contraction Primary murine lung fibroblasts Myofibroblast differentiation

ABSTRACT

Pulmonary fibrosis (PF) is a chronic progressive lung disease without effective medical treatment options leading to respiratory failure and death within 3–5 years of diagnosis. The pathological process of PF is driven by aberrant wound-healing involving fibroblasts and myofibroblasts differentiated by secreted profibrotic transforming growth factor β (TGF- β 1). Classical transient receptor potential 6 (TRPC6), a Na⁺- and Ca²⁺-permeable cation channel, is able to promote myofibroblast conversion of primary rat cardiac and human dermal fibroblasts and TRPC6-deficiency impaired wound healing after injury. To study a potential role of TRPC6 in the development of PF we analyzed lung function, gene and protein expression in wild-type (WT) and TRPC6-deficient (TRPC6-/-) lungs utilizing a bleomycin-induced PF-model. Fibrotic WT-mice showed a significant higher death rate while bleomycin-treated TRPC6-deficient mice were partly protected from fibrosis as a consequence of a lower production of collagen and an almost normal function of the respiratory system (reduced resistance and elastance compared to fibrotic WT-mice). On a molecular level TGF- β 1 induced TRPC6 up-regulation, increased Ca²⁺ influx and nuclear NFAT localization in WT primary murine lung fibroblasts (PMLFs) resulting in higher stress fiber formation and accelerated contraction rates as compared to treated TRPC6-deficient fibroblasts. Therefore, we conclude that TRPC6 is an important determinant for TGF- β 1-induced myofibroblast differentiation during fibrosis and specific channel inhibitors might be beneficial in a future treatment of PF.

© 2016 Elsevier B.V. All rights reserved.

1. Introduction

Idiopathic pulmonary fibrosis (IPF) is a chronic progressive lung disease leading to respiratory failure and death within 3–5 years of diagnosis [1]. Despite recent progress with the approval of pirfenidone and nintedanib for the treatment of IPF [2], the only curative treatment still is lung transplantation. The exact mechanism of IPF initiation and progression are still not well understood. Historically, inflammation has been postulated to injure alveolar units leading to progressive pulmonary fibrosis (PF), but multiple and potent anti-inflammatory therapies, particular corticosteroids have failed to show benefit in patients with IPF [3]. Now, a growing body of evidence reveals that the pathological process of IPF may be driven by aberrant wound-healing involving

E-mail address: Alexander.Dietrich@lrz.uni-muenchen.de (A. Dietrich).

fibroblasts and myofibroblasts differentiated by secreted profibrotic transforming growth factor β (TGF- β 1) [1,3,4]. IPF is indeed characterized by scattered accumulation of myofibroblasts in fibroproliferative foci and extracellular matrix deposition (e.g. collagen), which results in irreversible destruction of the lung architecture [1,4]. Many different cell types are able to transdifferentiate into activated fibroblasts and myofibroblasts including resident fibroblasts [5], type I and II alveolar epithelial cells [6,7], fibrocytes [8], pericytes [5] and pleural mesothelial cells [9].

Human and mouse classical transient receptor potential 6 (TRPC6) channels are members of the TRPC family (TRPC1–7) and are predominantly expressed in lung [10], [11]. Although Na⁺ and Ca²⁺ permeable cation channels of the TRPC family were the first cloned TRP channels in mammals, their functional importance is still poorly understood [12]. Among the TRPC channels, TRPC3, 6 and 7 share 69% identity and are gated by pathways involving receptor stimulated C-type phospholipases (PLCs) and activation by diacylglycerols (DAG) [10,13]. In

^{*} Corresponding author at: Walther-Straub-Institute of Pharmacology and Toxicology, Nußbaumstr. 26. 80336 Munich. Germany.

pulmonary smooth muscle cells TRPC6 is essential for acute hypoxic vasoconstriction [14] and regulates endothelial permeability inducing lung edema during ischemia-reperfusion injury [15].

Most interestingly, heterologous expression of TRPC6 in mouse embryonic, primary rat cardiac and primary human dermal fibroblasts promoted myofibroblast conversion in these cells [16]. Along these lines fibroblasts from TRPC6-deficient mice showed impaired wound healing after injury and were refractory to transforming growth factor (TGF- $\beta1$) which induces TRPC6 expression only in wild-type (WT) cells through p38 mitogen-activated protein kinases (MAPK) [16].

These and our own data prompted us to speculate about an important role of TRPC6 in differentiation of lung fibroblasts and progression of pulmonary fibrosis. We analyzed lung function, gene and protein expression in wild-type (WT) and TRPC6-deficient (TRPC6 -/-) lungs utilizing the well-established bleomycin-induced PF-model [17]. In TRPC6 -/- mice, collagen increase by PF induction was abrogated and lung function changes were significantly reduced in comparison to treated WT mice. On a cellular level, primary murine lung fibroblasts (PMLFs) from TRPC6-deficient mice pre-incubated with TGF- β 1 exposed a reduced contraction of a collagen matrix in clear contrast to WT cells, which showed increased TGF- β 1-induced TRPC6-expression. Therefore, we present for the first time evidence for a TRPC6-driven myofibroblast function contributing to PF development.

2. Materials and methods

2.1. Animals and bleomycin-induced pulmonary fibrosis

TRPC6 —/— mice were generated as previously described [18,19]. Eight- to twelve-week-old female C57BL/6N mice were used for all experiments and all animal experiments were approved by the governmental authorities (EU directive 2010/63/EU for animal experiments). Pulmonary fibrosis was induced by intra-tracheal application of 50 μ l bleomycin (3 U/kg/body weight). Bleomycin sulfate (Sigma-Aldrich, Taufkirchen, Germany) was dissolved in sterile PBS and applied using a MicroSprayer® Aerosolizer, Model IA-1C (Penn-Century, Wyndmoor, PA, USA). Control mice were treated with 50 μ l PBS. After instillation mice were kept for 14 days with free access to water and rodent laboratory chow.

2.2. Lung function

Mice were anesthetized with ketamine/xylazin, intratracheally intubated through a small incision of the trachea and connected to the flexiVent system (Scireq, Montreal, Canada).

2.3. Immunohistochemistry

After lung function measurement right lungs were excised and snapfrozen for protein analysis. The left lung was inflated with 4% (m/v) paraformaldehyde in PBS and processed for paraffin embedding. Paraffin-embedded tissue sections (3 µm) were cut using a microtome (Zeiss, Göttingen, Germany), mounted on glass slides, deparaffinized in xylene and rehydrated in graded alcohol. To asses fibrotic remodeling standard Trichrom Accustain staining by Lillie (Masson; Bouin's solution (Sigma)), Weigert's Iron Hematoxylin solution (Hematoxylin, Ironchloride-hexahydrate (Merck, Darmstadt, Germany)), Trichrome Stain (Masson) Kit (Biebrich Scarlet-Acid Fuchsin solution, Phosphomolybdic acid, Phosphotungstic acid, Aniline Blue; (Sigma, Taufkirchen, Germany), Acetic Acid) or standard hematoxylin and eosin (H&E; hematoxylin, eosin) was performed. After dehydration in increasing concentrations of alcohol, sections were mounted (Entellan; Merck, Darmstadt, Germany) and scanned with a Mirax Desk slide scanning device (Zeiss, Göttingen, Germany). Lungs of PBS treated control animals (WT n = 9, TRPC6 -/-n = 8) and bleomycin challenged (WT n = 7, TRPC6 -/-n = 8) were analyzed by IHC. Representative images are displayed in figures.

H&E stained tissue sections were analyzed by design-based stereology using an Olympus BX51 light microscope equipped with the new Computer Assisted Stereological Toolbox (newCAST, Visiopharm) as described [20] by readers blinded to the study groups. For mean chord length (MCL) measurements, 20 frames were selected randomly across multiple sections by the software, using the $\times 20$ objective, and superimposed by a line grid and points. The intercepts of lines on alveolar wall (Lsepta) and points localized on air space (Pair) were counted and calculated as MCL $= \sum Pair \times L(p) \, / \, \sum$ Isepta \times 0.5, where L(p) is the line length per point.

2.4. Quantification of collagen in isolated lungs

Lung collagen was quantified by analyzing hydroxyproline content in proteins using a high-pressure liquid chromatography (HPLC) method developed by Campa et al. [21] and modified by Mutsaers et al. [22]. Briefly, aliquots of powdered lung tissue were hydrolyzed in 6 M HCl at 110 °C for 16 h and an aliquot of the hydrolysate was dried at 55–60 °C. Hydroxyproline was isolated and measured by reverse phase HPLC after derivatization with 7-chloro-4-nitrobenz-2-oxa-1, 3-diazole (NBD-Cl; Sigma-Aldrich, Taufkirchen, Germany). Dried hydrolysates were reconstituted in 100 µl H₂O, buffered with 0.4 M potassium tetraborate (Sigma-Aldrich, Taufkirchen, Germany) and 12 mM NBD-Cl in methanol was added. Samples were incubated at 37 °C for 20 min in the dark. The reaction was stopped by 1.5 M HCl and finally 167 mM sodium acetate in acetonitrile (26% vol/vol) was added. 100 µl aliquots of the sample were loaded onto the column and eluted with an acetonitrile gradient. The hydroxyproline content in each sample was determined by comparing peak areas of samples with those from standard solutions.

2.5. Isolation and culture of primary murine lung fibroblasts

Primary murine lung fibroblasts (PMLF) were isolated as previously described for human lung fibroblasts [23]. Briefly, lungs of C57BL/6N mice were flushed through the right heart with sterile, cold PBS and excised. The lungs were dissected into pieces of 1–2 cm² in size and digested by 1 mg/ml of Collagenase I (Biochrom, Cambridge, UK) at 37 °C for 2 h. Digested lung pieces were filtered through a nylon filter (pore size 70 μ m; BD Falcon, Franklin Lakes, NJ, USA) and centrifuged for 5 min. Subsequently, the pellet was resuspended in DMEM/F12 fibroblast culture medium (Lonza, Basel, Switzerland) supplemented with 20% fetal bovine serum (Invitrogen, Carlsbad, USA) as well as penicillin/streptomycin (Lonza, Basel, Switzerland) and finally plated on 10 cm cell culture dishes.

Medium was changed after 2 days and cells were split after reaching a confluence of 80–90%. Only PMLFs from passage 4–9 were used for the studies.

2.6. TGF-β1 treatment of cultured PMLFs

Unless otherwise specified cells were grown to confluence and starved with 0.1% fetal bovine serum in DMEM/F12 for 24 h prior to TGF- β 1 treatment (2 ng/ml; R&D Systems, Minneapolis, MN, USA) or application of solvent for 48 h. All experiments were performed in DMEM/F12 medium supplemented with 0.1% FBS and antibiotics.

2.7. Quantitative reverse transcription (RT)-PCR analysis

Total RNA from primary lung fibroblasts and lung homogenate was isolated using an Invitrap® Spin Universal RNA Mini Kit (Invitek, Berlin, Germany). Real time PCR was done using the 2 × ABsolute™ QPCR SYBR Green Mix (Thermo Scientific, St. Leon-Rot, Germany). 10 pmol of each primer pair and 0.2 µl from the first strand synthesis were added to the

Table 1Primer pairs used for amplification of quantitative RT-PCR fragments.

Target	Species	Forward primer (5'-3')	Reverse primer (5'-3')
TRPC1	Mouse	TGA ACT TAG TGC TGA CTT AAA GGA AC	CGG GCT AGC TCT TCA TAA TCA
TRPC2	Mouse	CAC GAA AGG AGC CTG AGT TTA	CCA GCA ACT CGA AGC CAT AG
TRPC3	Mouse	TTA ATT ATG GTC TGG GTT CTT GG	TCC ACA ACT GCA CGA TGT ACT
TRPC4	Mouse	AAG GAA GCC AGA AAG CTT CG	CCA GGT TCC TCA TCA CCT CT
TRPC5	Mouse	ATG AGG GGC TAA CAG AAG A	TGC AGC CTA CAT TGA AAG
TRPC6	Mouse	GCA GCT GTT CAG GAT GAA AAC	TTC AGC CCA TAT CAT GCC TA
TRPC7	Mouse	CCT ACG CCA GGG ATA AGT G	AAG GCC ACA AAT ACC ATG A
AT1Ra	Mouse	ACT CAC AGC AAC CCT CCA AG	CTC AGA CAC TGT TCA AAA TGC AC
AT1Rb	Mouse	CAG TTT CAA CCT CTA CGC CAG T	GGG TGG ACA ATG GCT AGG TA
IL-6	Mouse	ACT TCA CAA GTC CGG AGA GG	TGC CAT TGC ACA ACT CTT TTC
MCP-1	Mouse	CTT CTG GGC CTG CTG TTC A	CCA GCC TAC TCA TTG GGA TCA
KC	Mouse	CCG AAG TCA TAG CCA CAC	GTG CCA TCA GAG CAG TCT
β-Actin	Mouse	CTA AGG CCA ACC GTG AAA AG	ACC AGA GGC ATA CAG GGA CA
HPRT	Mouse	CCT AAG ATG AGC GCA GTT GAA	CCA CAG GAC TAG AAC ACC TGC TAA

reaction mixture and PCR was carried out in a light-cycler apparatus (Roche, Mannheim, Germany) using the following conditions: 15 min initial activation and 45 cycles of 12 s at 94 °C, 30 s at 50 °C, 30 s at 72 °C. Primers pairs from Table 1 were used for the amplification of specific DNA-fragments from the first strand synthesis. Fluorescence intensities were recorded after the extension step at 72 °C after each cycle. Samples containing primer dimers were excluded by melting curve analysis and identification of the products by agarose gel electrophoresis. Crossing points were determined by the software program provided by the manufacturer. Relative gene expression was quantified using the formula: $(2e^{(Crossing point reference gene - Crossing point X)}) \times 100 = % of reference gene expression or the difference between both crossing points (<math>\Delta$ CP).

2.8. Collagen gel contraction assay

Fibroblasts at 70% confluency were harvested and resuspended in DMEM/F12 with 0.1% FBS. Fibroblasts were then seeded into collagen matrices (150,000 Fibroblasts per well of a 24-well plate). Culture medium (DMEM/F12 with 0.1% FBS and antibiotics) containing TGF- β 1 (2 ng/ml dissolved in 0.1% BSA in PBS) or control buffer (solvent of TGF- β 1) was added on top of each polymerized collagen lattice and cultures were incubated for 2 days. The collagen gels were released from the edges and the surfaces areas were calculated using ImageJ software (NIH).

2.9. Quantification of nuclear NFAT

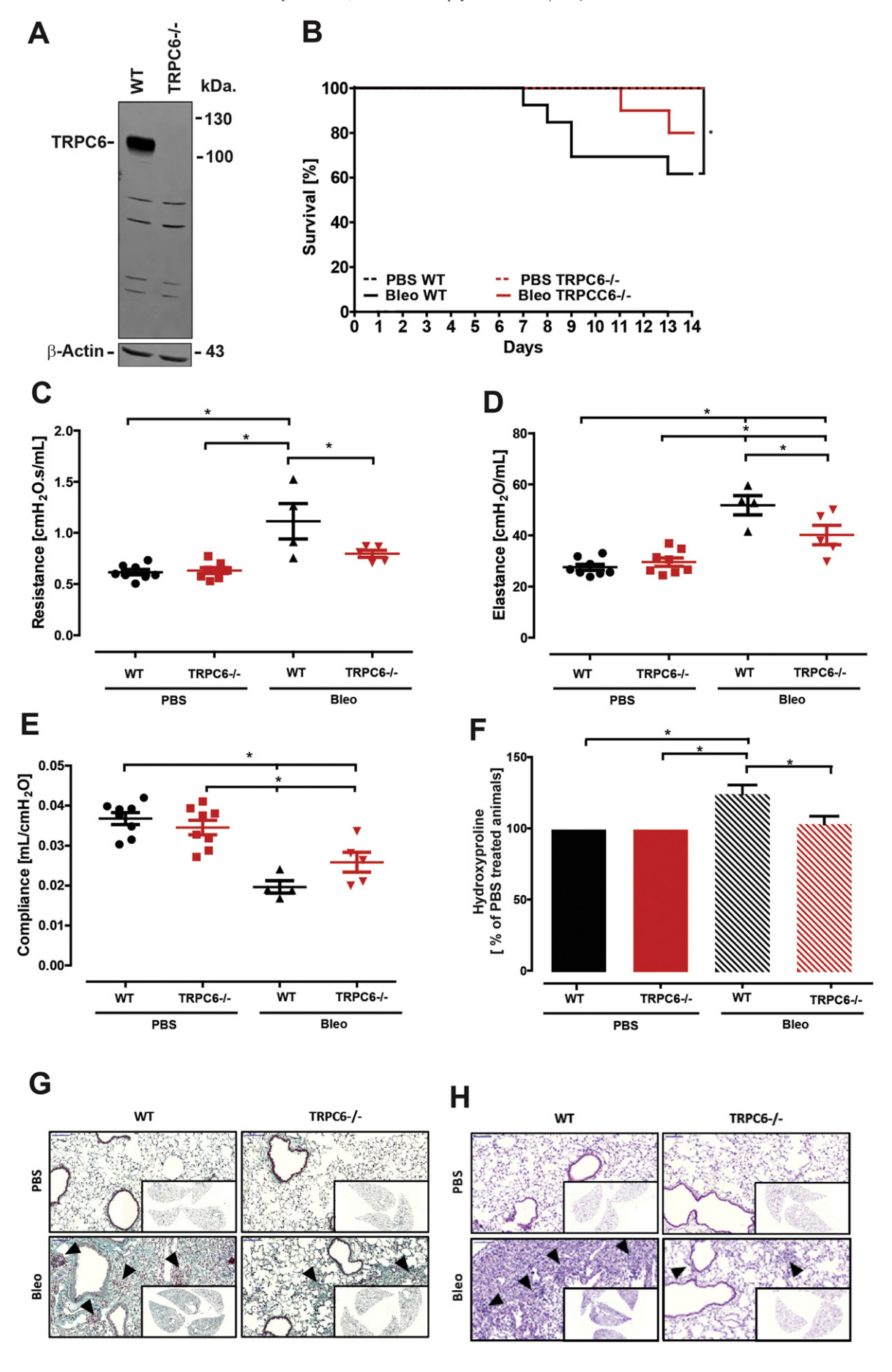
Isolation of nuclear protein extracts from PMLF treated with TGF- $\beta 1$ or solvent was performed with a Nuclear Extract Kit according to the manufacturer's instructions (Active Motif, 40010, La Hulpe, Belgium). In brief, cells were first washed with PBS containing phosphatase inhibitors. Cytoplasmic protein fractions were collected by adding hypotonic lysis buffer and detergent, causing leakage of cytoplasmic proteins into the supernatant. After centrifugation (14.000 $\times g$ for 30 s) nuclear protein fractions were obtained by resuspending pellets in detergent-free lysis buffer containing protease inhibitors. NFAT proteins were analyzed by Western Blotting as described below using an NFATc1 specific antiserum and lamin B1 antibodies as loading control. Protein bands were

normalized to loading controls and quantified by an Odyssey Fc system (Licor, Lincoln, USA).

2.10. Western blot analysis

Cells from 20 cm cell culture dishes were washed two times with PBS and 250 µl of lysis buffer (20 mM Tris-HCL, pH 7.5, 150 mM NaCl, 1% Nonidet P40, 0.5% sodium deoxycholate, 1% SDS, 5 mM EDTA) was applied for 30 min at 4 °C. After centrifugation of the protein lysates at 5500×g for 30 min at 4 °C protein concentration was quantified using a BCA-Assay (Pierce, Thermo Fisher, Schwerte, Germany) according to the manufacturer's instructions. $6 \times$ Laemmli buffer (375 mM $4 \times$ Tris/ SDS buffer, pH 6.8, 48% glycerin, 6% SDS, 0,03% bromophenol blue and 9% β-mercaptoethanol) was added, the mixture incubated at 90 °C for 10 min and sonicated for 15 s. 14 µg protein of each sample was loaded on a 10% SDS gel. Protein separation was performed at room temperature using a current of 20 mAmp for 2-3 h. To transfer the proteins to a PVDF membrane a current of 20 mA was applied for 20 h at 4 °C. After transfer, the membrane was rinsed with 10 ml PBST for 5 min at room temperature. Transfer was checked using Ponceau solution (A2935 0500, AppliChem, Darmstadt, Germany). Blocking was performed for 1 h at room temperature using 10 ml blocking buffer (5% low fat milk in PBST). Each primary antibody was diluted in PBST containing 0.05% sodium azide according to the manufacturer's protocol and applied over night at 4 °C. After washing with PBST three times for 10 min each, HRP-conjugated secondary antibody was applied for 2 h at room temperature. The membrane was washed with PBST three times, for 10 min each and incubated in Super Signal West Dura chemiluminescent substrate (34075, Thermo Scientific, Waltham, MA, USA). Chemiluminescence was detected by exposure of the filter to Carestream BioMax Light films (8194540, Kodak) or in an Odyssey®Fc unit (Licor, Lincoln, NE, USA). Used antibodies and dilutions were: HRP-conjugated anti-β-actin antibody (Sigma A3854HRP, 1:10,000); anti-αSMA antibody (mouse, Sigma-Aldrich A2547, 1:2000); anti-vinculin antibody (mouse, Sigma V9131, 1:10,000); anti-TRPC6 antibody (rabbit AK 861 affinity purified, 1:200); Anti-NFATc1 (mouse, Santa Cruz Biotechnology sc-7294, 1:600); Anti-Lamin B1 (rabbit, Thermo Scientific PA5-19468, 1:5000); secondary anti-mouse-IgG HRP-linked antibody (Cell Signaling #7076, 1:2000), and secondary anti-rabbit IgG peroxidase (POX)-antibody (Sigma A6154, 1:10,000).

Fig. 1. TRPC6-deficiency protects mice from bleomycin-induced pulmonary fibrosis. (A) TRPC6 protein expression was evaluated in whole lung lysates of wildtype (WT) and TRPC6-deficient (TRPC6-/-) mice by immunoblotting using a specific antiserum. (B) Survival curves of PBS-treated control (WT, n=9; TRPC6-/-, n=8) and Bleomycin (Bleo) treated WT (n=13) and TRPC6-/- mice (n=10) from day 0 to day 14 after the application. (C-E) function measurements of the respiratory system (C, resistance; D, elastance, E, compliance) of control and bleomycin-treated WT and TRPC6-deficient mice. (F) Quantification of hydroxproline as an indicator for lung collagen, in acid hydrolysates of pulverized lung tissue (WT PBS, n=9; TRPC6-/- PBS, n=8; WT Bleo n=6; TRPC6-/- Bleo n=7). (G) Representative Masson's Trichrome staining of lung sections from bleomycin-treated WT and TRPC6-deficient mice. Scale bars $2\times = 1000 \, \mu m$, $20\times = 100 \, \mu m$ (H) Representative hematoxylin and eosin (H&E) staining of lung sections from bleomycin-treated WT and TRPC6-deficient mice. Scale bars $2\times = 1000 \, \mu m$, $20\times = 100 \, \mu m$. Data are expressed as mean \pm SEM. *, P<0.05. The log-rank (Mantel-Cox)-test was used for comparison of survival distributions in B.



2.11. Analysis of extracellular matrix proteins by immunohistochemistry

Cells were seeded on 18 × 18 mm cover slips and grown until confluence, washed three times with PBS and incubated in 3.7% formaldehyde for 15 min at room temperature for fixation. Formaldehyde was removed by rinsing with PBS for three times and permeabilization was performed for 10 min in 0.5% Triton X-100 in PBS followed by blocking for 1 h at room temperature using a mixture of 4% BSA and 4% goat serum in PBS. All antibodies were diluted in blocking buffer according to the manufacturer's protocol. Primary antibodies were incubated overnight at 4 °C. After rinsing three times with PBS for 5 min each, secondary antibody was applied for 1 h. Samples were washed again three times with PBS for 5 min each. To counterstain cell nuclei an additional staining with Hoechst 33342 (Life Technologies, Darmstadt, Germany) was applied. Used antibodies and dilutions were: anti α -smooth muscle actin (α-SMA) antibody (mouse, Sigma A2547, 1:2000), anti fibronectin (Fn1) antibody (rabbit, Santa Cruz sc-9068, 1:50), anti collagen1a1 (Coll1a1) antibody (rabbit, Rockland 600-401-103-0.1, 1:50) and secondary antibodies anti mouse-FITC (Sigma F9006, 1:80) and anti rabbit-Alexa488 (Life Technologies, A11008, 1:500). Detection was made using fluorescence microscopy (Olympus, Hamburg, Germany).

2.12. Phalloidin staining of actin stress fibres

Polymerized actin filaments were stained with Phalloidin-TRITC (Sigma-Aldrich, Taufkirchen, Germany) according to the manufacturer's protocols. To counterstain cell nuclei an additional incubation with Hoechst 33342 (Life Technologies, Darmstadt, Germany) was performed. Sample preparation and visualization was carried out as described in the previous paragraph. Greyscale quantification was done with software provided by Olympus (Olympus, Hamburg, Germany).

2.13. Intracellular Ca²⁺ measurements

PMLF from WT and TRPC6 —/— mice were analyzed from three independent preparations of mice (WT or TRPC6 —/—). Cells in passage 4 were seeded on 25 mm coverslips and treated as described (see Section 2.6). PMLF on coverslips were loaded with fura-2-acetoxymethylester (5 μ M) in 0.1% BSA in HBSS buffer at 37 °C for 20 min. Coverslips were then placed on the microscope in a low-volume recording chamber with HBSS buffer. Calcium influx was induced by the membrane-permeable diacylglycerol (DAG)-analogue 1-oleyl-2-acetyl-sn-glycerol (OAG) which was diluted in 0.1% BSA in HBSS. Cytosolic calcium increases (Ca^{2+} influx) were recorded using a Polychrome V monochromator (Till Photonics, Martinsried, Germany) and a 14-bit EMCCD camera (iXON3 885, Andor, Belfast, UK) coupled to an inverted microscope (IX71 with an UPlanSApo 20×/0.85 oil immersion objective, Olympus, Hamburg, Germany) at 340 and 380 nm for quantification of $[Ca^{2+}]_i$.

2.14. Statistical analysis

Results are shown as mean \pm SEM. Differences between groups were analyzed using t-tests, two-way-analysis of variance (ANOVA) and log-rank (Mantel-Cox)-test as proposed by a commercial software program (GraphPad Prism).

3. Results

3.1. TRPC6-deficient mice are partially protected from fibrotic effects of bleomycin

To study a potential role of TRPC6 in PF we analyzed survival rates, lung function and collagen secretion in wild-type (WT) and TRPC6-deficient (TRPC6-/-) mice after intra-tracheal application of bleomycin or PBS. As demonstrated in Fig. 1A only WT mice express TRPC6 protein

in their lungs. Both WT and TRPC6-deficient mice showed a significant weight loss from day 4 after application of bleomycin, in clear contrast to control mice of both genotypes treated with PBS (Suppl. Fig. 1). These data indicate no significant changes in the health status of WT and TRPC6-deficient mice during the initial inflammatory phase after bleomycin treatment. Moreover, cytokine (IL-6, KC, MCP-1) levels in lung homogenates were not different in control and treated WT and TRPC6 —/— lungs (Supplementary Fig. 2A, B, C). After day seven however, only bleomycin-treated WT mice revealed significantly lower survival rates than PBS-treated WT mice as indicated in the Kaplan-Meier plot in Fig. 1B. Although we detected no significant difference in survival rates comparing WT and TRPC6 -/- mice after injury using the suggested statistical tests for the Kaplan-Meyer plot, there is a clear trend towards an earlier onset of death in WT mice compared to TRPC6 -/mice. After day 14 we tested the function of the respiratory system in the remaining mice. Importantly, the resistance of the respiratory system as a characteristic hallmark of lung fibrosis was not increased in bleomycin treated TRPC6—/— mice as compared to bleomycin treated WT mice and similar to PBS treated WT and TRPC6 -/- mice (Fig. 1C). The elastance of the respiratory system was significantly reduced in TRPC6-deficient mice compared to bleomycin-treated WT mice (Fig. 1D). While we observed no significant changes in the compliance of the respiratory system in bleomycin treated animals, there was a clear trend towards increased compliance in the TRPC6-deficient animals (Fig. 1E). Notably, quantification of hydroxyproline by HPLC analysis (Fig. 1F) revealed that collagen levels were significantly increased in bleomycin treated WT mice, but not in TRPC6-deficient mice, which exhibited similar collagen contents as PBS-treated control animals. Masson's Trichrom (Fig. 1G) and hematoxylin (Fig. 1H) staining of lung sections showed the typical patchy pattern of fibrotic plaques in bleomycin-treated animals, which were decreased in TRPC6-deficient mice (Fig. 1G, H). Mean cord lengths in lung sections which are increased during the development of emphysema were not significantly different in mice of all genotypes treated with PBS or bleomycin (Bleo) (Supplementary Fig. 3). In summary these data demonstrate a partial protection of TRPC6-deficient mice from bleomycin-induced lung fibrosis.

3.2. Isolation and characterization of primary lung fibroblasts (PMLF) from WT and TRPC6-deficient mice reveals no phenotypic differences

To investigate the role of TRPC6 on a cellular level, we isolated primary murine lung fibroblasts (PMLF) from WT and TRPC6-deficient mice. PMLF were identified by staining with α -smooth muscle actin (α -SMA), fibronectin 1 (Fn1) and collagen (Coll1a1) (Fig. 2A for WT fibroblasts and Supplementary Fig. 5 for TRPC6 —/— fibroblasts). We did not observe any obvious differences in the cell structure between the both genotypes (Fig. 2B). As TRPC6 deficiency might be compensated for by upregulation of closely related members of the TRPC family [18], we assessed the expression of TRPC transcripts in primary PMLF. Quantitative reverse-transcription PCR analysis revealed predominant expression of TRPC1 mRNA only in PMLF of both genotypes (Fig. 2C). A compensatory up- or down-regulation of other TRPC mRNAs (TRPC1-5, 7) in TRPC6-deficient PMLF was not observed (Fig. 2C).

3.3. TRPC6-deficient primary lung fibroblasts differentiated to myofibroblasts by TGF-\(\beta\)1 express lower levels of actin stress fibers

After incubation of WT-PMLF with TGF- β 1 (2 ng/ml) for 48 h application of 1-oleyl-2-acetyl-sn-glycerol (OAG) as a direct activator of TRPC6 increased intracellular Ca²⁺ levels to a significantly higher extent as in untreated WT and TRPC6 —/— cells as well as in TGF- β 1—treated TRPC6 deficient cells (Fig. 3A). Quantitative RT-PCR revealed a significant 3fold upregulation of TRPC6 mRNA in WT but not in TRPC6-deficient TGF- β 1 differentiated myofibroblasts (Fig. 3B). While protein expression of TRPC6 was induced in WT PMLF by application of TGF-

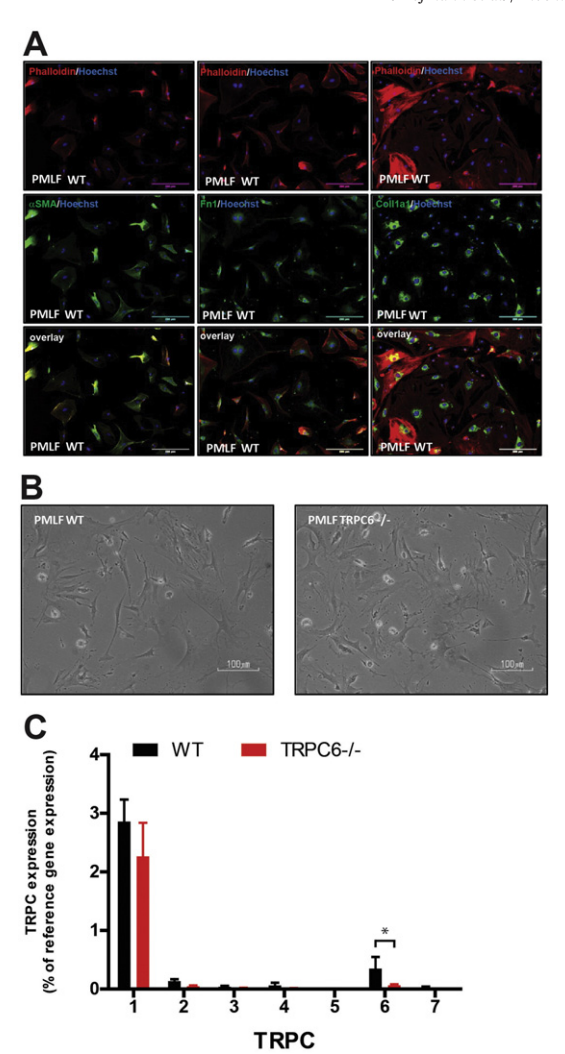


Fig. 2. Identification of TRPC-expression in primary murine lung fibroblasts isolated from WT and TRPC6 —/— mice. (A) Representative images of immunofluorescence stained WT PMLFs incubated with fluorescence-coupled antibodies directed against specific fibroblast marker proteins (Fibronectin1/Fn1, α -smooth muscle actin/ α SMA, Collagen type1a1/Coll1a1). Scale bar = 200 μ m. (B) Representative phase contrast images of WT and TRPC6 —/— PMLFs. (C) Relative mRNA amounts of TRPC channels (TRPC1–5, 7) in WT and TRPC6 —/— PMLFs analyzed by quantitative RT-PCR (WT, n=5 mice; TRPC6—/— n=4 mice).

β1, TRPC6 protein was not detectable in naive PMLF of both genotypes and in TGF-β1-treated TRPC6 —/— cells (Fig. 3C). In contrast to cardiac and dermal fibroblasts [16], however, angiotensin II (AngII) had no effects on TRPC6 levels in WT fibroblasts (Supplementary Fig. 4A), although angiotensin receptor 1 (AT1Ra, AT1Rb see Supplementary Fig. 4B and [24]) and angiotensin receptor 2 [24] are expressed in primary murine lung fibroblasts. Immunohistochemical analysis of TRITC-phalloidin binding revealed significant higher numbers of actin stress fibers in TGF-β1 differentiated WT myofibroblasts, which was reduced in TRPC6 —/— cells (Fig. 3D, E).

3.4. TRPC6-deficient primary lung fibroblasts carry less nuclear factor of activated T-cells c1 (NFATc1) in their nuclei after application of TGF- β 1 compared to WT cells

To evaluate the consequences of decreased Ca²⁺ influx in TRPC6 —/— fibroblasts we quantified nuclear NFATc1 isoforms (Fig. 4A) after application of TGF-β1 or solvent. The fold increase of nuclear NFATc1 isoforms after incubation with TGF-β1 was significantly higher in WT fibroblasts compared to TRPC6 —/— fibroblasts (Fig. 4B),

indicating that TRPC6-induced Ca²⁺ influx is responsible for calcineurin-mediated dephosphorylation and nuclear translocation of NFATc1 as described for cardiac (myo)fibroblasts [16].

3.5. TRPC6-deficient primary lung fibroblasts differentiated to myofibroblasts by TGF-\(\beta\)1 showed less contraction of a collagen matrix

To analyze contraction of a collagen gel matrix as a primary function of myofibroblasts, primary fibroblasts of both genotypes were cultured in collagen matrices and incubated in TGF- $\beta 1$ or in control medium. After releasing collagen matrices TGF- $\beta 1$ -treated fibroblasts showed significant higher contractions in comparison to untreated fibroblasts (Fig. 4C). Basal contractions of untreated TRPC6-deficient cells were significantly lower than in untreated WT cells, and TGF- $\beta 1$ -treatment of TRPC6-/- cells only induced contractions similar to untreated WT cells (Fig. 4D). The reason for the lower basal contraction of TRPC6-/- fibroblasts independently of TGF- $\beta 1$ is unknown and needs further investigation. We concluded that TRPC6-deficiency reduces basal contraction of fibroblasts which is not rescued in TGF- $\beta 1$ -differentiated myofibroblasts.

4. Discussion

For the first time we present evidence for an important role of TRPC6 in myofibroblast function in vitro and progression of PF in vivo. TRPC6deficient mice were protected in a bleomycin-induced PF model as evidenced by an unchanged survival rate as compared to PBS-treated control TRPC6 —/— mice. Bleomycin-treated WT mice, however, showed significantly reduced survival rates in comparison to PBS-treated WT mice. Most parameters of lung function as well as collagen contents in TRPC6 —/— were similar to PBS-treated control mice (Fig. 1). While no major morphological changes were detected in primary murine lung fibroblasts (PMLF) from WT and TRPC6 -/- mice (Fig. 2), TGFβ1 induced TRPC6 expression and OAG activated Ca²⁺ influx only in WT PMLF (Fig. 3A-C). Moreover, TGF-β1-induced actin stress fiber formation was significantly reduced in TRPC6-/- myofibroblasts (Fig. 3D, E). Basal cell contraction of (myo)fibroblasts as characteristic hallmark of PF progression [20,25] was decreased in TRPC6 —/— cells compared to their WT control cells (Fig. 4). These findings highlight the role of TRPC6 in the formation of PF.

The bleomycin-induced mouse model is an established in vivo model for lung fibrosis [26]. We applied this model to initially determine the in vivo relevance of TRPC6 on the development of PF. After an inflammatory phase in the first seven days following application of bleomycin, accompanied by weight loss of the animals, a fibrotic phase characterized by an increased death rate ensues. We detected no difference in survival rates and weight loss in control WT and TRPC6 -/- mice, while significantly more bleomycin-treated WT mice than PBS-treated WT mice died during the fibrotic phase. TRPC6 —/— mice subjected to bleomycin showed significantly improved lung function parameters in comparison to fibrotic WT mice with levels similar to untreated mice. Both bleomycin treated WT and TRPC6 –/– mice lose weight during the first seven days of inflammation in this fibrosis model and do not recover weight in the next seven days. We assume that there is no direct correlation between body weight and lung phenotype on these days. However, this issue deserves further investigation. Importantly, collagen production was unchanged in bleomycin-treated TRPC6deficient lungs, but increased in bleomycin-treated WT mice. Encouraged by these results we isolated primary lung fibroblasts to analyze these differences in genotypes on the cellular and molecular

It is generally accepted that fibroblasts mainly contribute to the progression of PF by regulating ECM turnover and by their differentiation to myofibroblasts [27–29], although they are not the only cell type involved in the disease [30–32]. TGF- β 1 secreted by epithelial or inflammatory cells activates fibroblasts by stimulating ECM production and

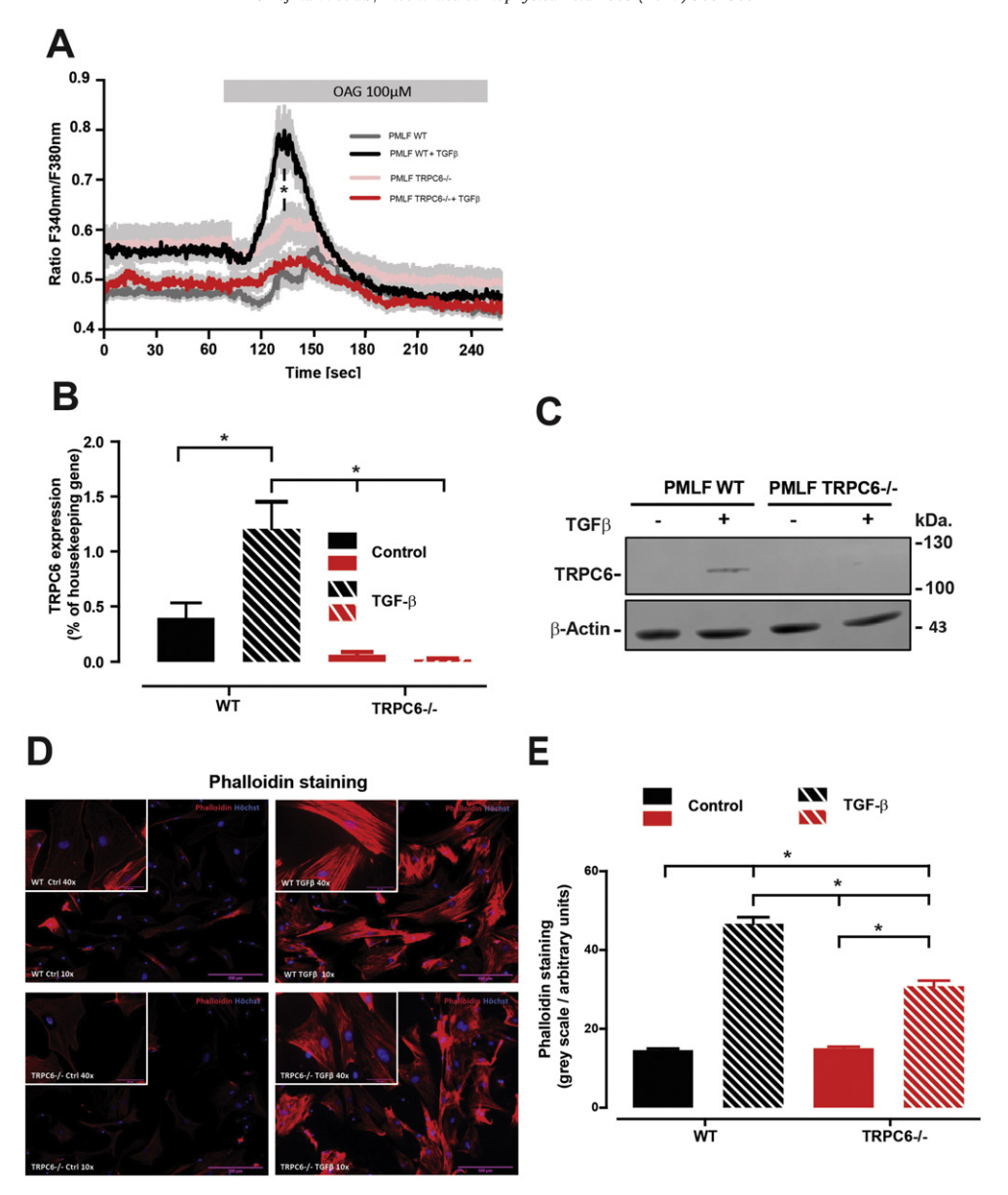


Fig. 3. Characterization of fibroblasts and TGF- β 1 induced myofibroblasts from TRPC6 —/— and WT mice. Primary murine lung fibroblasts (PMLFs) isolated from WT and TRPC6 —/— mice were grown until confluence and incubated for 48 h with TGF- β 1 (2 ng/ml) or solvent. (A) OAG (1-oleyl-2-acetyl-sn-glycerol)-mediated increases in intracellular Ca²⁺ ([Ca²⁺]_i) in WT (n=40 cells) and TRPC6—deficient fibroblasts (n=19 cells) and myofibroblast (WT, n=53 cells from 3 mice; TRPC6—/—, n=38 cells from 3 mice) after application of TGF- β 1. [Ca²⁺]_i levels were detected by analysis of fluorescence ratios (Ratios 340/380 nm). Lines represent calculated means and light grey areas indicate standard error of the mean (SEM) of three experiments. The asterisk marks significant differences (P < 0.05) between ratios of WT cells after application of TGF- β 1 and ratios of all other analyzed cells. (B) mRNA expression of TRPC6 in control and TGF- β 1-treated WT and TRPC6—/— cells (n=5 each) was determined by reverse-transcription (RT)-quantitative PCR and normalized to a housekeeping gene. (C) TRPC6 expression was evaluated in whole cell lysates of WT and TRPC6—/— PMLF by immunoblotting using specific antibodies. (D) Representative images of immunofluorescence staining of WT and TRPC6—/— PMLFs with Phalloidin before and after application of TGF- β 1. (E) Quantification of phalloidin staining. Data are expressed as mean ± SEM. *, P < 0.05.

initiating myofibroblast differentiation, leading to a more contractile phenotype [29,33–35]. This contractile phenotype was clearly reduced in TRPC6 —/— fibroblasts differentiated to myofibroblasts as actin stress fibers were significantly decreased and cell contractility was inhibited in a collagen gel matrix. Contraction is essential for cell motility [36] and important for invasion of myofibroblasts into fibrotic plaques [37]. These data clearly indicate that TRPC6 plays an important role in myofibroblasts corroborating results reported in dermal and cardiac fibroblasts [16]. The authors proposed a Ca²⁺/TRPC6-dependent calcineurin A (CnA) activation of nuclear factor of activated T cells (NFAT) initiating a serum response factor (SRF)-driven fibroblast myofibroblast transformation [16]. We are now presenting clear evidence for a TGF- β 1-induced TRPC6 expression in pulmonary myofibroblasts and a TRPC6-dependent increase in intracellular Ca²⁺, nuclear NFAT

localization, collagen production and contraction which promotes pulmonary fibrosis and decreases lung function in PF (see graphical abstract online). Moreover, TRPC6 might be an important biomarker for myofibroblast differentiation, because its expression is up-regulated in TGF-β1-induced myofibroblasts. Our data however do not exclude functions of TRPC6 in other cell types important for PF progression e.g. fibrocytes [30,32], pericytes [38], endothelial [39] and epithelial cells [31] which is under further investigation in our laboratory.

While this work was in progress another member of the TRP superfamily was identified as an important player in the development of pulmonary fibrosis in mice [40]. TRP vanilloid 4 (TRPV4) is a non-selective cation channel that was originally identified as an osmosensor in *C. elegans* [41–43] and is ubiquitously expressed in various cell types including fibroblasts [40]. TRPV4-deficient mice like TRPC6 —/— mice

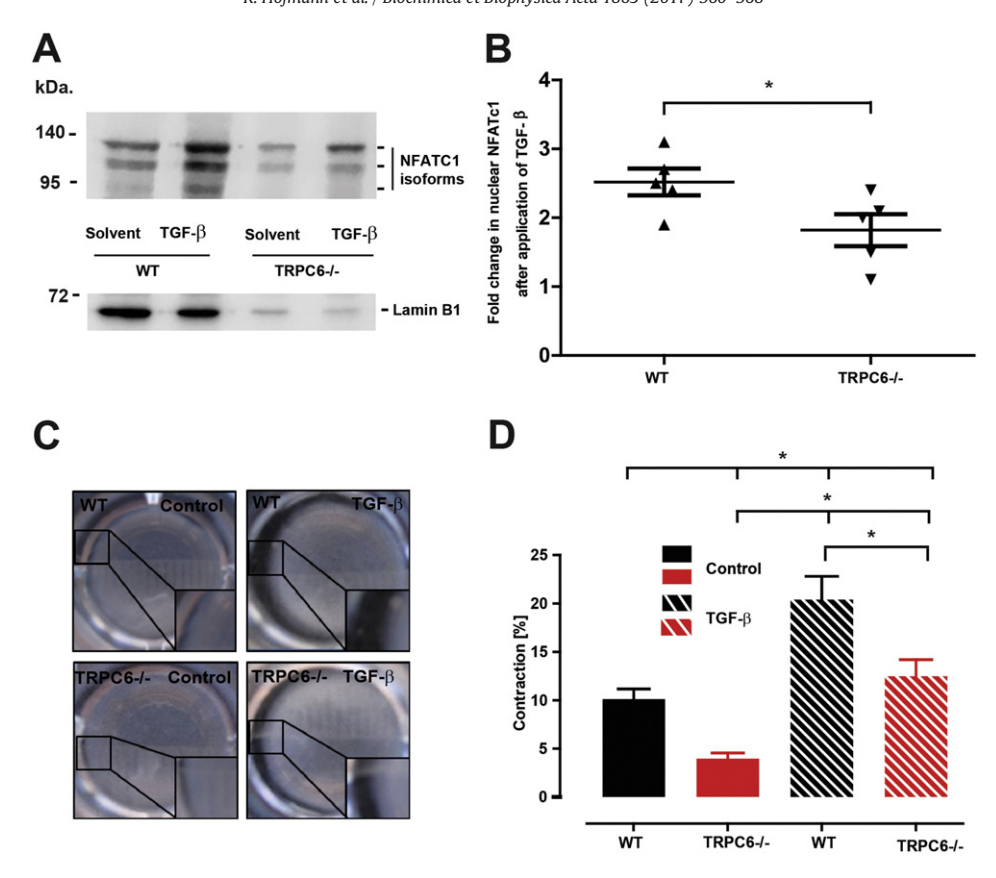


Fig. 4. Analysis of TGF- β 1-induced NFAT translocation to nuclei and contraction of myofibroblasts. (A) Upper panel: NFATc1 isoforms detected in WT and TRPC6 -/- fibroblast nuclei after incubation of the cells with solvent or TGF- β 1 for 48 h. Lower panel: Lamin B1 as loading control was used for normalization, (B) fold increase of nuclear NFATc1 after incubation with TGF- β 1 in wild-type (WT) and TRPC6 -/- (TRPC6 -/-) fibroblast nuclei. (C) Representative photographs of floating collagen gel matrices seeded with PMLFs (WT and TRPC6 -/-) and incubated with TGF- β 1 (2 ng/ml) or solvent after release from the well edges. Insets show areas of gel contraction. (D) Summary of data obtained in the gel matrix contraction assay (n=6 experiments). Data are expressed as mean \pm SEM. *, P<0.05.

were protected from bleomycin-induced lung fibrosis and TRPV4 channel activity was elevated if cells were plated on matrices of increasing stiffness. Its role in lung fibroblasts however is clearly different from TRPC6 function identified by us. TRPV4 is not upregulated by TGF-\\Beta1 but works independently of this pathway and is activated by matrix stiffness induced by already initiated ECM secretion [40]. Therefore, TRPV4 up-regulated in patients with severe PF might be important for the final steps in progression of the disease, while TRPC6 is essential for PF initiation. Most importantly, TRPC6 —/— myofibroblasts show reduced contraction in a collagen matrix assay essential for cell migration to the fibrotic plaques which is beneficial for gas exchange in the alveoli. Comparable results have not been reported for TRPV4-/myofibroblasts so far. For both TRPV4 [44] and TRPC6 [45,46] channel inhibitors were identified. An orally applied TRPV4 blocker with low IC₅₀ values between 2 and 40 nM was already effective in the treatment of pulmonary edema [44]. Larixyl derivatives block TRPC6 twelve fold more effective than its closely related TRPC3 channels with IC₅₀ values of 100-600 nM [46]. Most interestingly, acute hypoxic pulmonary vasoconstriction in mouse lungs which is initiated by TRPC6 activity [14] was completely blocked by 5 µM of larixylacetate [46]. Therefore, testing both inhibitors in mouse models of pulmonary fibrosis will be very promising and a first step for future therapeutic approaches of PF with specific TRP channel inhibitors.

Supplementary data to this article can be found online at http://dx.doi.org/10.1016/j.bbadis.2016.12.002.

Transparency document

The Transparency document associated with this article can be found, in online version.

Acknowledgments

We would like to thank Bettina Braun, Rabea Imker and Anastasia van den Berg (CPC) for excellent technical assistance and Sarah Hampe and Susanna Zierler for help with NFATc1 immunoblots. This work was funded by the Deutsche Forschungsgemeinschaft (TRR 152, Project 16).

References

- T.E. King Jr., A. Pardo, M. Selman, Idiopathic pulmonary fibrosis, Lancet 378 (2011) 1949–1961.
- [2] A.S. Selvaggio, P.W. Noble, Pirfenidone initiates a new era in the treatment of idiopathic pulmonary fibrosis, Annual Review of Medicine, 2015.
- [3] M. Selman, T.E. King, A. Pardo, Idiopathic pulmonary fibrosis: prevailing and evolving hypotheses about its pathogenesis and implications for therapy, Ann. Intern. Med. 134 (2001) 136–151.
- [4] B. Hinz, S.H. Phan, V.J. Thannickal, M. Prunotto, A. Desmouliere, J. Varga, O. De Wever, M. Mareel, G. Gabbiani, Recent developments in myofibroblast biology: paradigms for connective tissue remodeling, Am. J. Pathol. 180 (2012) 1340–1355.
- [5] C. Hung, G. Linn, Y.H. Chow, A. Kobayashi, K. Mittelsteadt, W.A. Altemeier, S.A. Gharib, L.M. Schnapp, J.S. Duffield, Role of lung pericytes and resident fibroblasts in the pathogenesis of pulmonary fibrosis, Am. J. Respir. Crit. Care Med. 188 (2013) 820–830.
- [6] K.K. Kim, M.C. Kugler, P.J. Wolters, L. Robillard, M.G. Galvez, A.N. Brumwell, D. Sheppard, H.A. Chapman, Alveolar epithelial cell mesenchymal transition develops in vivo during pulmonary fibrosis and is regulated by the extracellular matrix, Proc. Natl. Acad. Sci. U. S. A. 103 (2006) 13180–13185.
- [7] H. Tanjore, D.S. Cheng, A.L. Degryse, D.F. Zoz, R. Abdolrasulnia, W.E. Lawson, T.S. Blackwell, Alveolar epithelial cells undergo epithelial-to-mesenchymal transition in response to endoplasmic reticulum stress, J. Biol. Chem. 286 (2011) 30972–30980.
- [8] N. Hashimoto, H. Jin, T. Liu, S.W. Chensue, S.H. Phan, Bone marrow-derived progenitor cells in pulmonary fibrosis, J. Clin. Invest. 113 (2004) 243–252.
- [9] K.K. Mubarak, A. Montes-Worboys, D. Regev, N. Nasreen, K.A. Mohammed, I. Faruqi, E. Hensel, M.A. Baz, O.A. Akindipe, S. Fernandez-Bussy, S.D. Nathan, V.B. Antony, Parenchymal trafficking of pleural mesothelial cells in idiopathic pulmonary fibrosis, Eur. Respir. J. 39 (2012) 133–140.

- [10] T. Hofmann, A.G. Obukhov, M. Schaefer, C. Harteneck, T. Gudermann, G. Schultz, Direct activation of human TRPC6 and TRPC3 channels by diacylglycerol, Nature 397 (1999) 259–263.
- [11] G. Boulay, X. Zhu, M. Peyton, M. Jiang, R. Hurst, E. Stefani, L. Birnbaumer, Cloning and expression of a novel mammalian homolog of Drosophila transient receptor potential (Trp) involved in calcium entry secondary to activation of receptors coupled by the Gq class of G protein, J. Biol. Chem. 272 (1997) 29672–29680.
- [12] B. Nilius, G. Owsianik, The transient receptor potential family of ion channels, Genome Biol. 12 (2011) 218.
- [13] T. Okada, R. Inoue, K. Yamazaki, A. Maeda, T. Kurosaki, T. Yamakuni, I. Tanaka, S. Shimizu, K. Ikenaka, K. Imoto, Y. Mori, Molecular and functional characterization of a novel mouse transient receptor potential protein homologue TRP7. Ca(2+)-permeable cation channel that is constitutively activated and enhanced by stimulation of G protein-coupled receptor, J. Biol. Chem. 274 (1999) 27359–27370.
- [14] N. Weissmann, A. Dietrich, B. Fuchs, H. Kalwa, M. Ay, R. Dumitrascu, A. Olschewski, U. Storch, M. Mederos y Schnitzler, H.A. Ghofrani, R.T. Schermuly, O. Pinkenburg, W. Seeger, F. Grimminger, T. Gudermann, Classical transient receptor potential channel 6 (TRPC6) is essential for hypoxic pulmonary vasoconstriction and alveolar gas exchange, Proc. Natl. Acad. Sci. U. S. A. 103 (2006) 19093–19098.
- [15] N. Weissmann, A. Sydykov, H. Kalwa, U. Storch, B. Fuchs, M. Mederos y Schnitzler, R.P. Brandes, F. Grimminger, M. Meissner, M. Freichel, S. Offermanns, F. Veit, O. Pak, K.H. Krause, R.T. Schermuly, A.C. Brewer, H.H. Schmidt, W. Seeger, A.M. Shah, T. Gudermann, H.A. Ghofrani, A. Dietrich, Activation of TRPC6 channels is essential for lung ischaemia-reperfusion induced oedema in mice, Nat. Commun. 3 (2012) 649.
- [16] J. Davis, A.R. Burr, G.F. Davis, L. Birnbaumer, J.D. Molkentin, A TRPC6-dependent pathway for myofibroblast transdifferentiation and wound healing in vivo, Dev. Cell 23 (2012) 705–715.
- [17] K. Williams, J. Roman, Studying human respiratory disease in animals role of induced and naturally-occurring models, J. Pathol. (2015).
- [18] A. Dietrich, Y.S.M. Mederos, M. Gollasch, V. Gross, U. Storch, G. Dubrovska, M. Obst, E. Yildirim, B. Salanova, H. Kalwa, K. Essin, O. Pinkenburg, F.C. Luft, T. Gudermann, L. Birnbaumer, Increased vascular smooth muscle contractility in TRPC6—/— mice, Mol. Cell. Biol. 25 (2005) 6980–6989.
- [19] M. Suzuki, A. Mizuno, K. Kodaira, M. Imai, Impaired pressure sensation in mice lacking TRPV4, J. Biol. Chem. 278 (2003) 22664–22668.
- [20] G. John-Schuster, K. Hager, T.M. Conlon, M. Irmler, J. Beckers, O. Eickelberg, A.O. Yildirim, Cigarette smoke-induced iBALT mediates macrophage activation in a B cell-dependent manner in COPD, Am. J. Physiol. Lung Cell. Mol. Physiol. 307 (2014) 1692–1706.
- [21] J.S. Campa, R.J. Mcanulty, G.J. Laurent, Application of high-pressure liquid-chromatography to studies of collagen production by isolated cells in culture, Anal. Biochem. 186 (1990) 257–263.
- [22] S.E. Mutsaers, M.L. Foster, R.C. Chambers, G.J. Laurent, R.J. McAnulty, Increased endothelin-1 and its localization during the development of bleomycin-induced pulmonary fibrosis in rats, Am. J. Respir. Cell Mol. Biol. 18 (1998) 611–619.
- [23] C.A. Staab-Weijnitz, I.E. Fernandez, L. Knuppel, J. Maul, K. Heinzelmann, B.M. Juan-Guardela, E. Hennen, G. Preissler, H. Winter, C. Neurohr, R. Hatz, M. Lindner, J. Behr, N. Kaminski, O. Eickelberg, FK506-binding protein 10, a potential novel drug target for idiopathic pulmonary fibrosis, Am. J. Respir. Crit. Care Med. 192 (2015) 455-467
- [24] M. Konigshoff, A. Wilhelm, A. Jahn, D. Sedding, O.V. Amarie, B. Eul, W. Seeger, L. Fink, A. Gunther, O. Eickelberg, F. Rose, The angiotensin II receptor 2 is expressed and mediates angiotensin II signaling in lung fibrosis, Am. J. Respir. Cell Mol. Biol. 37 (2007) 640–650.
- [25] E.S. White, Lung extracellular matrix and fibroblast function, Ann. Am. Thorac. Soc. 12 (Suppl. 1) (2015) S30–S33.

- [26] B.B. Moore, C.M. Hogaboam, Murine models of pulmonary fibrosis, American journal of physiology, Lung Cell. Mol. Physiol. 294 (2008) L152–L160.
- [27] R.J. McAnulty, Fibroblasts and myofibroblasts: their source, function and role in disease, Int. J. Biochem. Cell Biol. 39 (2007) 666–671.
- [28] B. Hinz, Formation and function of the myofibroblast during tissue repair, J. Invest. Dermatol. 127 (2007) 526–537.
- [29] C.J. Scotton, R.C. Chambers, Molecular targets in pulmonary fibrosis: the myofibroblast in focus, Chest 132 (2007) 1311–1321.
- [30] R.M. Strieter, E.C. Keeley, M.A. Hughes, M.D. Burdick, B. Mehrad, The role of circulating mesenchymal progenitor cells (fibrocytes) in the pathogenesis of pulmonary fibrosis, J. Leukoc. Biol. 86 (2009) 1111–1118.
- [31] M. Konigshoff, P. Bonniaud, Live and let die: targeting alveolar epithelial cell proliferation in pulmonary fibrosis, Am. J. Respir. Crit. Care Med. 190 (2014) 1339–1341.
- [32] S. Maharaj, C. Shimbori, M. Kolb, Fibrocytes in pulmonary fibrosis: a brief synopsis, Eur. Respir. Rev. 22 (2013) 552–557.
- [33] U. Bartram, C.P. Speer, The role of transforming growth factor beta in lung development and disease, Chest 125 (2004) 754–765.
- [34] W.I. de Boer, A. van Schadewijk, J.K. Sont, H.S. Sharma, J. Stolk, P.S. Hiemstra, J.H. van Krieken, Transforming growth factor beta1 and recruitment of macrophages and mast cells in airways in chronic obstructive pulmonary disease, Am. J. Respir. Crit. Care Med. 158 (1998) 1951–1957.
- [35] K.F. Chung, Cytokines in chronic obstructive pulmonary disease, Eur. Respir. J. Supplement 34 (2001) 50s–59s.
- [36] A. Pathak, S. Kumar, From molecular signal activation to locomotion: an integrated, multiscale analysis of cell motility on defined matrices, PLoS One 6 (2011), e18423.
- [37] B. Hinz, The myofibroblast: paradigm for a mechanically active cell, J. Biomech. 43 (2010) 146–155.
- [38] J.E. Rowley, J.R. Johnson, Pericytes in chronic lung disease, Int. Arch. Allergy Immunol. 164 (2014) 178–188.
- [39] L. Farkas, D. Farkas, K. Ask, A. Moller, J. Gauldie, P. Margetts, M. Inman, M. Kolb, VEGF ameliorates pulmonary hypertension through inhibition of endothelial apoptosis in experimental lung fibrosis in rats, J. Clin. Invest. 119 (2009) 1298–1311.
- [40] S.O. Rahaman, L.M. Grove, S. Paruchuri, B.D. Southern, S. Abraham, K.A. Niese, R.G. Scheraga, S. Ghosh, C.K. Thodeti, D.X. Zhang, M.M. Moran, W.P. Schilling, D.J. Tschumperlin, M.A. Olman, TRPV4 mediates myofibroblast differentiation and pulmonary fibrosis in mice, J. Clin. Invest. 124 (2014) 5225–5238.
- [41] R. Strotmann, C. Harteneck, K. Nunnenmacher, G. Schultz, T.D. Plant, OTRPC4, a non-selective cation channel that confers sensitivity to extracellular osmolarity, Nat. Cell Biol. 2 (2000) 695–702.
- [42] W. Liedtke, Molecular mechanisms of TRPV4-mediated neural signaling, Ann. N. Y. Acad. Sci. 1144 (2008) 42–52.
- [43] J. Vriens, H. Watanabe, A. Janssens, G. Droogmans, T. Voets, B. Nilius, Cell swelling, heat, and chemical agonists use distinct pathways for the activation of the cation channel TRPV4, Proc. Natl. Acad. Sci. U. S. A. 101 (2004) 396–401.
- [44] K.S. Thorneloe, M. Cheung, W. Bao, H. Alsaid, S. Lenhard, M.Y. Jian, M. Costell, K. Maniscalco-Hauk, J.A. Krawiec, A. Olzinski, E. Gordon, I. Lozinskaya, L. Elefante, P. Qin, D.S. Matasic, C. James, J. Tunstead, B. Donovan, L. Kallal, A. Waszkiewicz, K. Vaidya, E.A. Davenport, J. Larkin, M. Burgert, L.N. Casillas, R.W. Marquis, G. Ye, H.S. Eidam, K.B. Goodman, J.R. Toomey, T.J. Roethke, B.M. Jucker, C.G. Schnackenberg, M.I. Townsley, J.J. Lepore, R.N. Willette, An orally active TRPV4 channel blocker prevents and resolves pulmonary edema induced by heart failure, Sci. Transl. Med. 4 (2012) (159ra148).
- [45] N. Urban, K. Hill, L. Wang, W.M. Kuebler, M. Schaefer, Novel pharmacological TRPC inhibitors block hypoxia-induced vasoconstriction, Cell Calcium 51 (2012) 194–206.
- 46] N. Urban, L. Wang, S. Kwiek, J. Rademann, W.M. Kuebler, M. Schaefer, Identification and validation of larixyl acetate as a potent TRPC6 inhibitor, Mol. Pharmacol. 89 (2016) 197–213.